

運輸省港湾技術研究所

# 港湾技術研究所 報告

---

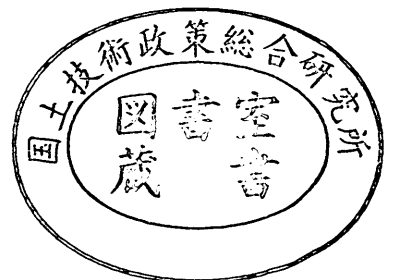
---

REPORT OF  
THE PORT AND HARBOUR RESEARCH  
INSTITUTE  
MINISTRY OF TRANSPORT

---

VOL. 27      NO. 2      JUNE 1988

NAGASE, YOKOSUKA, JAPAN



# 港湾技術研究所報告 (REPORT OF P.H.R.I.)

第27巻 第2号 (Vol. 27, No. 2), 1988年6月 (June 1988)

## 目 次 (CONTENTS)

1. Stability Analysis of Geotechnical Structures by Adaptive Finite Element Procedure  
..... Masaki KOBAYASHI ..... 3  
(適応有限要素法による地盤の安定解析.....小林正樹)
2. 改良型波力発電ケーソン防波堤の特性  
——波エネルギーに関する研究, 第7報—— ...高橋重雄・安達 崇・田中 智..... 23  
(Stability and Function of Improved-type Wave Power Extracting Caisson Breakwater  
——A Study on Development of Wave Power, 7th Rept.——  
.....Shigeo TAKAHASHI, Takashi ADACHI and Satoru TANAKA)
3. 現地観測データを用いた方向スペクトル推定法に関する検討  
..... 橋本典明・小舟浩治・亀山 豊..... 59  
(Examination of the Various Directional Spectral Estimation Methods for  
Field Wave Data.....Noriaki HASHIMOTO, Koji KOBUNE and Yutaka KAMEYAMA)
4. 海象観測用船型ブイの運動特性に関する模型実験と現地観測  
..... 高山智司・平石哲也・高山 優・甲斐源太郎・中埜岩男・古賀道明..... 95  
(Model Tests and Field Observation on Motions of a Ship-shaped Buoy for  
Marine Observation .....Tomotsuka TAKAYAMA, Tetsuya HIRAISHI, Masaru  
TAKAYAMA, Gentaro KAI, Iwao NAKANO and Michiaki KOGA)
5. 深層混合処理工法による改良体に作用する外力  
..... 寺師昌明・北誥昌樹・中村 健.....147  
(External Forces Acting on a Stiff Soil Mass Impoved by DMM  
.....Masaaki TERASHI, Masaki KITAZUME and Takeshi NAKAMURA)
6. アスファルトコンクリートの老化性状..... 佐藤勝久・八谷好高・阿部洋.....185  
(Changes in Properties of Asphalt Concretes due to Aging  
..... Katsuhisa SATO, Yoshitaka HACHIYA and Yoichi ABE)
7. 剛基礎上の重力式係船岸の地震時滑動量推定手法の実験的研究  
..... 上部達生・守屋正平・工藤勝己.....211  
(An Experimental Study on Estimation Procedures of Seismic Sliding Displacements  
for the Gravity Type Quaywall on the Rigid Base  
..... Tatsuo UWABE, Masahira MORIYA and Katsumi KUDO)
8. CFRP ロッドを緊張材としたアンボンド PC 梁の曲げ性状  
..... 大即信明・山本邦夫・浜田秀則.....241  
(Bending Behavior of Unbonded Prestressed Concrete Beams Prestressed with  
CFRP Rods ..... Nobuaki OTSUKI, Kunio YAMAMOTO and Hidenori HAMADA)

# 1. Stability Analysis of Geotechnical Structures by Adaptive Finite Element Procedure

Masaki KOBAYASHI\*

## Synopsis

A new method of stability analysis for geotechnical structures has been developed by using the finite element method including the adaptive procedure.

The bearing capacity of strip footings was analyzed by this method. The results agree favourably with the classical bearing capacity equations.

The stability of simple slopes was analyzed and was compared with conventional results by Taylor. The finite element method appears to give higher safety factors in frictional slopes whereas it gives favourable agreement with the results of the conventional method in cohesive slopes.

The effect of a sheet pile on the stability of a slope was analyzed to show the powerful capabilities of the finite element method. The increase of the stability due to the existence of a sheet pile can be analyzed. The effect of its flexural rigidity also can be evaluated.

To improve the results of the finite element method, the adaptive procedure was applied to the limit analysis. Extremely accurate results can be obtained by the adaptive procedure both in the bearing capacity analysis and in the slope stability analysis.

**Key Words:** Stability Analysis, Finite Element Method, Slope Stability, Bearing Capacity

---

\* Chief of Soil Mechanics Laboratory, Soils Division

# 1. 適応有限要素法による地盤の安定解析

小林 正樹\*

## 要 旨

有限要素法によって安定解析を行う方法を開発した。この方法を用いて、地盤の支持力と斜面安定の問題を解析した。その結果によると、有限要素法による極限支持力は厳密解にほぼ近い値を与えている。また、斜面安定においては、 $\phi=0$ の場合には有限要素法の値はTaylorの結果とよく一致したが、 $\phi \neq 0$ の場合には有限要素法による安全率の値がTaylorによる値より大きな傾向がみられた。

今回開発した方法を用いて、矢板のすべり防止効果の問題を解析した。この場合、矢板の根入れ長さ、矢板の剛性が地盤の安定性に及ぼす影響を評価できることが明らかになった。

さらに、誤差評価を行いその結果に基づきメッシュ再分割を行う、適応有限要素法によって支持力および斜面安定の解析を行い、非常に精度の高い解析結果が得られることを明らかにした。

キーワード：安定解析，有限要素法，支持力，斜面安定

---

\* 土質部 土性研究室長

## Contents

|   |    |
|---|----|
| <b>Synopsis</b> .....                             | 3  |
| <b>1. Introduction</b> .....                      | 7  |
| <b>2. Limit Analysis by Finite Elements</b> ..... | 7  |
| 2.1 Mechanical model of soil .....                | 7  |
| 2.2 Computational procedure .....                 | 8  |
| 2.3 Numerical examples .....                      | 8  |
| <b>3. Adaptive Refinement</b> .....               | 14 |
| 3.1 Error estimate and Adaptive analysis .....    | 14 |
| 3.2 Numerical examples .....                      | 15 |
| <b>4. Conclusion</b> .....                        | 19 |
| <b>References</b> .....                           | 21 |

## 1. Introduction

Limit analysis such as bearing capacity, slope stability and earth pressure has been one of the most important subjects in geotechnical engineering. Conventional methods are usually employed for the limit analysis. For example, classical closed form solutions are frequently used to obtain the ultimate bearing capacity and the circular slip method is the most popular one used in the slope stability analysis. However, there are many problems where we have a lot of difficulties in applying conventional methods.

Recently, it was shown that the finite element method can be applied to the limit analysis if a careful algorithm is employed. Although usual finite element approach fails to give the accurate limit value, fictitious viscoplastic algorithm<sup>1)</sup> yields satisfactory results. However, the comparison of the finite element solutions with the closed form solutions shows that relatively high limit values are obtained in the finite element analysis where the high stress singularities exist. One typical example is the bearing capacity problem of a footing whose edge causes stress singularity. Another example is the stability problem of a vertical slope where stress singularities are seen at the corner. One useful method to divert these stress singularities is the introduction of a singular finite element. However, the application of this element is limited to the stress singular point and the overall accuracy cannot be estimated.

Recently the application of the adaptive refinement procedure has become popular in the finite element analysis. In this method, mesh refinements are carried out based on the error estimate. Because of the difficulties in incorporating the whole refinement procedures into usual computer codes, the application of the mesh refinement analysis has been limited to a few problems. Zienkiewicz et al. developed a new algorithm of the error estimate which can be easily applied to the usual finite element method. However, their algorithm cannot be directly used for the limit analysis because its application is limited to the linear elastic problems. The author extended the algorithm to non-linear problems.

In this report, at first, we show that the finite element method has powerful capabilities for the limit analysis. Then, we demonstrate that extremely accurate limit analysis is made possible by the non-linear adaptive finite element procedure.

## 2. Limit Analysis by Finite Elements

### 2.1 Mechanical model of soil

Conventional limit analysis in soil mechanics employs the Mohr-Coulomb yield criterion whose strength parameters are defined as the cohesion  $c$  and the angle of shear resistance  $\phi$ . Therefore, in the finite element analysis we also use the Mohr-Coulomb yield criterion. However, soil is assumed to be elasto-plastic material in the finite element analysis although rigid plastic theory is used in conventional limit analyses. In the rigid plastic analysis, the yield or failure criterion consisting of only two parameters  $c$  and  $\phi$  suffice to describe the mechanical model. On the other hand, in the elasto-plastic analysis we have to determine four parameters, i.e.,  $c$ ,  $\phi$ , Young's modulus  $E$  and Poisson's ratio  $\nu$ . Furthermore, the concept of the plastic potential and the hardening rule are necessary in the elasto-plastic analysis. Usually, the plastic potential is assumed to be identical to the yield function (associated flow rule) and the strain hardening is neglected (perfect plasticity). Therefore, four parameters given above suffice to describe the elasto-plastic material employed in the finite element analysis.

Although two shear strength parameters  $c$  and  $\phi$  are familiar to most geotechnical

engineers, other two parameters  $E$  and  $\nu$  are seldom used in soil mechanics. Thus, there may be a lot of difficulties in determining  $E$  and  $\nu$ . However, we need not be worried about how to determine  $E$  and  $\nu$  because they have a negligible influence on the results of the limit analysis as will be shown below.

## 2.2 Computational procedure

In the limit analysis, we have to obtain ultimate values or safety factors. It is straightforward to get the ultimate value such as the ultimate bearing capacity. For example, we can calculate the ultimate bearing capacity of a rigid footing by increasing nodal displacements on the footing and by summing up the nodal reactions on the footing. However, to obtain such safety factors as calculated in the slope stability analysis, we have to devise a special algorithm. A simple and yet effective algorithm is to assume that computational divergence is equivalent to the total failure in soil mechanics. In this algorithm, shear strength  $\tau_f$  is reduced by a factor of  $F$  and the mobilized strength  $\tau_m$  is obtained as follows:

$$\tau_m = \tau_f / F$$

If a computational value converges under the condition of  $\tau_m$ , the safety factor must be greater than  $F$ . On the other hand, if the solution never converges after a large number of iterations, the safety factor is assumed to be less than  $F$ . We start a computation at a small value of  $F$  where the convergence is guaranteed. By increasing  $F$  which means a gradual reduction of shear strength parameters, we can obtain a point at which the solution no longer converges. The safety factor is given as  $F$  at this point.

In this analysis, it is essential to accurately judge whether a solution converges or not. If the solution diverges because of the drawbacks of the computational algorithm, we have unreasonable results. Recently, a new algorithm has been developed to analyze elasto-plastic problems. Here a fictitious elasto-viscoplastic analysis is performed instead of the simple incremental elasto-plastic analysis. It is shown that very stable and accurate limit value can be obtained by this new algorithm. In this report, we applied this algorithm to the Mohr-Coulomb material. The details of computational procedure are described in Appendix.

## 2.3 Numerical examples

### (1) Bearing capacity of strip footing

To show that the finite element method has powerful capabilities for the limit analysis, we obtained the ultimate bearing capacity of a strip footing. According to the classical bearing capacity theory, the ultimate bearing capacity  $q_d$  is given by

$$q_d = cN_c + 0.5B N_\gamma + qN_q$$

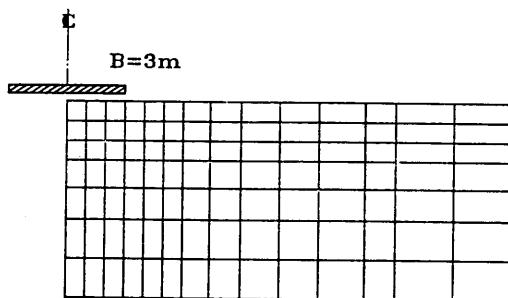


Fig. 1 Mesh division for bearing capacity analysis (original mesh)

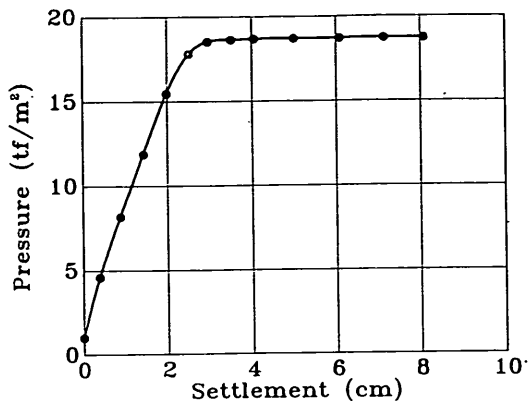


Fig. 2 Load-settlement relationship  
( $\phi = \gamma = q = 0$ )

where  $c$  is the cohesion,  $\gamma$  is the unit weight of soil,  $B$  is the footing width,  $q$  is the surcharge and  $N_c$ ,  $N_\gamma$ ,  $N_q$  are bearing capacity factors.

In the finite element analysis, these three bearing capacity factors are obtained separately and compared with those in the bearing capacity theory. Figure 1 shows the finite element mesh used in the bearing capacity analysis. 8 noded quadratic isoparametric elements are employed throughout in this report. The footing is assumed to be infinitely rigid. The following Elastic constants were used in the analysis:  $E = 20000$  tf/m<sup>2</sup> and  $\nu = 0.35$ .

At first the bearing capacity factor  $N_c$  for  $\phi = 0$  was calculated. Figure 2 shows the result of the load-settlement relationship. In the conventional incremental elasto-plastic finite element analysis, the load increases gradually even at a extremely large settlement. Thus, it is difficult to define the ultimate load. On the other hand, as shown in Fig. 2, it is very easy to obtain the ultimate bearing capacity because a peak value of the load is observed clearly in the elasto-viscoplastic analysis.

In the elasto-plastic finite element analysis, we have to use the elastic constants  $E$  and  $\nu$  together with the shear strength parameters  $c$  and  $\phi$ . To examine the influences of the elastic constants in the finite element analysis, the values of  $N_c$  for  $\phi = 0$  was calculated for various  $E$  and  $\nu$  as listed in Table 1. As shown in this table, elastic constants have a negligible effect except when  $\nu$  approaches quite near to 0.5. Thus, it was shown that the fictitious viscoplastic finite element analysis can give reliable bearing capacity factors.

The bearing capacity factors  $N_c$ ,  $N_q$ , and  $N_\gamma$  for various values of  $\phi$  were

Table 1 Effect of elastic constants on bearing capacity factor  $N_c$

| $E$       | $\nu$ | $N_c$ |
|-----------|-------|-------|
| 200       | 0.35  | 5.42  |
| 20,000    | 0.35  | 5.42  |
| 2,000,000 | 0.35  | 5.42  |
| 20,000    | 0     | 5.41  |
| 20,000    | 0.45  | 5.44  |
| 20,000    | 0.499 | 5.54  |



calculated with two footing conditions; smooth footings and rough footings. The mesh is the same as shown in Fig. 1. The same elastic constants were used as in Fig. 2;  $E=20000 \text{ tf/m}^2$  and  $\nu=0.35$ . The results of the finite element analysis were compared with the classical bearing capacity equations.

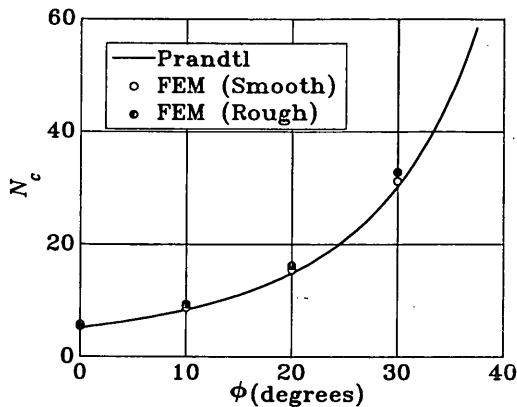


Fig. 3 Relationship between  $N_c$  and  $\phi$

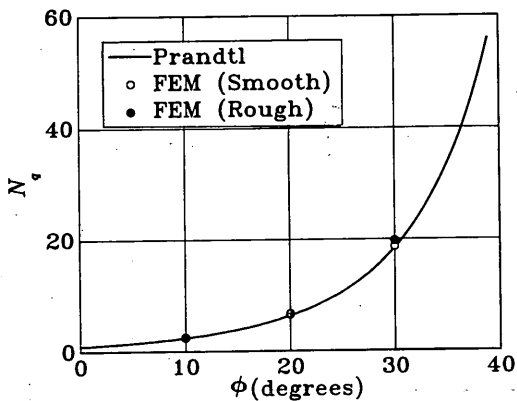


Fig. 4 Relationship between  $N_q$  and  $\phi$

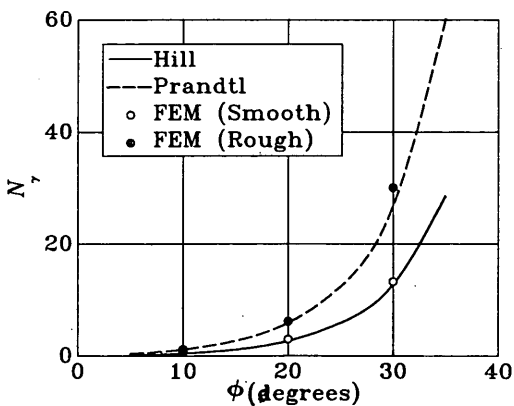


Fig. 5 Relationship between  $N_\gamma$  and  $\phi$

Figure 3 shows the relationship between  $N_c$  and  $\phi$ . In this figure, the values of  $N_c$  for a smooth footing are shown as open circles and those for rough footing are shown as closed circles for the finite element results. According to Prandtl, the values of  $N_c$  for both smooth footing and rough footing are the same as shown as the solid curve in Fig. 3. Although the finite element analysis gives a little differences in  $N_c$  between the smooth footing and the rough footing, the overall accuracy appears to be quite satisfactory.

Figure 4 shows the relationship between the bearing capacity factor  $N_q$  and the angle of shear resistance  $\phi$ . In this figure, similarly to  $N_c$ , the finite element solutions for both the smooth footing and the rough footing are shown together with the

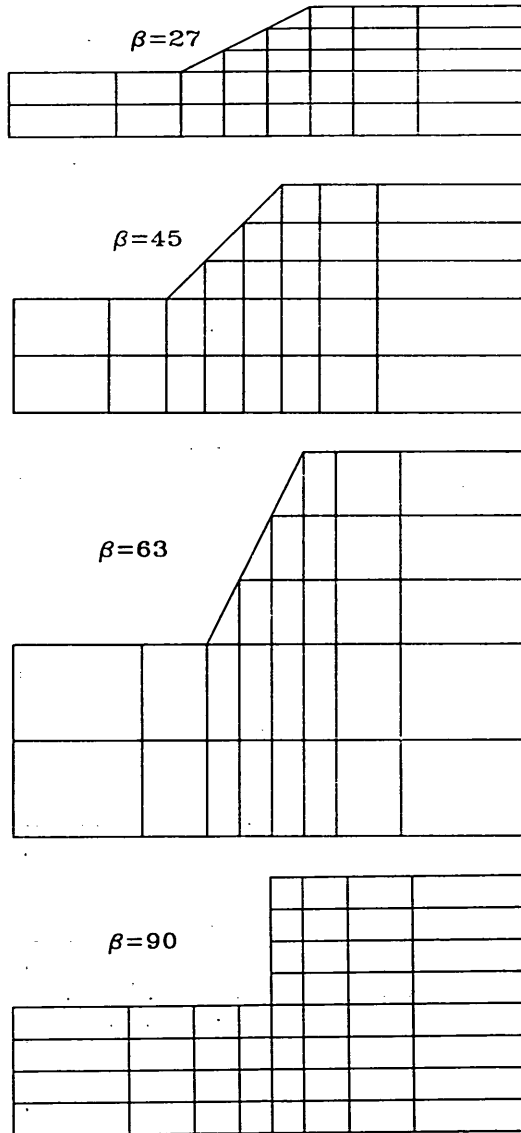


Fig. 6 Mesh division for slope stability analysis (original mesh)

theory due to Prandtl who confirmed that the values of  $N_q$  for the smooth footing is the same as that for the rough footing. The finite element analysis again gives satisfactory results.

Figure 5 shows the relationship between the bearing capacity factor  $N_\gamma$  and the angle of shear resistance  $\phi$ . In this figure, the finite element solutions for both the smooth footing and the rough footing are compared. It should be noted that we have quite different values of  $N_\gamma$  depending on the footing roughness. In fact, it is impossible to calibrate the solutions obtained by the finite element analysis because there is no closed form solution for  $N_\gamma$ . The slip line analysis by Chen<sup>2)</sup> gives similar differences in  $N_\gamma$ . He assumed that the Hill type failure mechanism holds for the smooth footing and the Prandtl type failure mechanism holds for the rough footing, respectively. In Fig. 5, the results of his analysis are compared with those by the finite element analysis, which gives reasonable results.

(2) Slope stability analysis

In this section, a slope stability analysis was performed for simple slopes having simple geometric conditions and a uniform soil condition. The finite element analysis was carried out for four slopes whose angles of inclination range from 27° to 90°. Figure 6 shows the element mesh of each slope. Safety factors were calculated by the finite element method and the results were compared with those by the conventional stability charts.

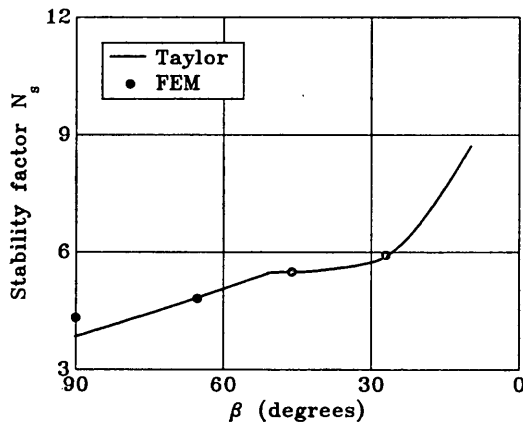


Fig. 7 Relationship between  $N_s$  and  $\beta(\phi=0)$

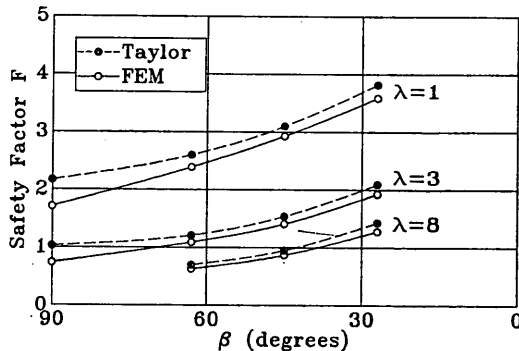


Fig. 8 Relationship between  $N_s$  and  $\beta(\phi>0)$

At first, the stability analysis was carried out for the case of  $\phi=0$ . Figure 7 shows the comparison of the stability factors  $N_s$  derived by the finite element method and those by the Taylor's stability chart<sup>3</sup>. In this figure, the stability factors are plotted against the slope inclination  $\beta$ . As shown in this figure, the finite element analysis gives very accurate results except when  $\beta=90^\circ$ .

Subsequently, similar comparison was made for the case of  $\phi>0$ . Figure 8 shows the results. In this figure, the relationship between the safety factor  $F$  and  $\beta$  are given for three  $\lambda$  values;  $\lambda$  is the nondimensional parameter given by  $\lambda = \gamma H \tan \phi / c$  where  $H$  is the slope height. It is clear that the finite element analysis gives slightly larger safety factors than the Taylor's stability chart. The difference is the largest when  $\beta=90^\circ$ .

(3) Effect of sheet pile in preventing slope failures

As was described above, the finite element method can give almost as accurate results as conventional methods in the limit analysis. To show further capabilities of the finite element analysis in the limit analysis, another computation is carried out on the effect of sheet piles in preventing slope failures.

Figure 9 shows a vertical slope consisting of two clay layers with different shear strength. We can expect that failure may be prevented if a sheet pile is driven deep enough to the lower clay layer because the lower clay has quite high strength compared with the upper clay. Conventional limit analysis fails to give satisfactory results for this kind of problem. The finite element analysis can give a reasonable safety factor even for this kind of problem because the computational procedure is the same as for simple slopes.

Figure 10 shows the relationship between the safety factor and the depth of

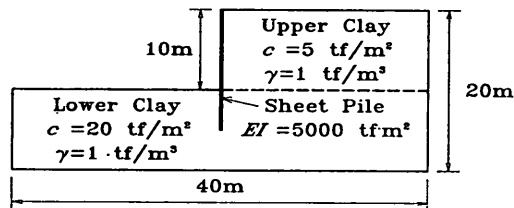


Fig. 9 Analysis of effect of sheet pile in preventing slope failure

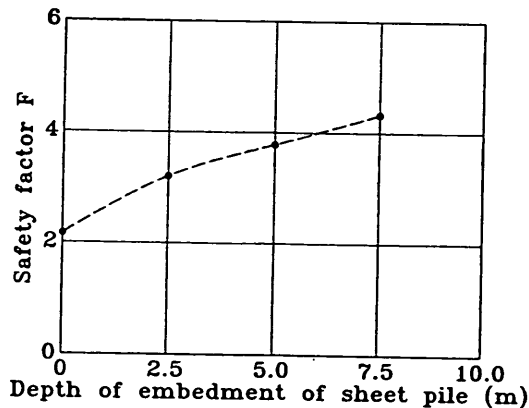


Fig. 10 Relationship between safety factor and depth of embedment

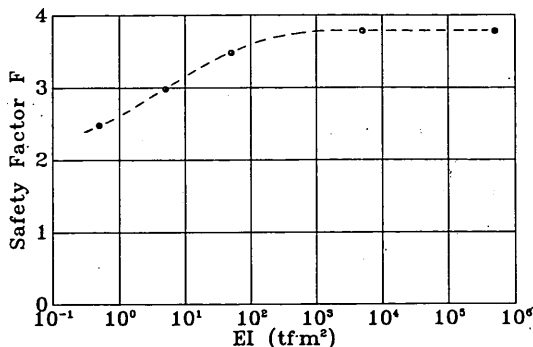


Fig. 11 Relationship between safety factor and flexural rigidity

embedment of a sheet pile. In this analysis, the sheet pile is assumed to be a linear elastic material with flexural rigidity  $EI=5000 \text{ tf}\cdot\text{m}^2$ . Different elastic constants are used for the clays;  $E=10000 \text{ tf}/\text{m}^2$  for the upper clay and  $E=4000 \text{ tf}/\text{m}^2$  for the lower clay with  $\nu=0.49$  for both clays. As shown in Fig. 10, the overall safety factor of this slope increases with the increase of the depth of the sheet pile. By conventional methods, it is almost impossible to obtain this kind of tendency. Although the sheet pile is assumed to be linear elastic in this analysis, we can obtain further satisfactory results by assuming a sheet pile as elasto-plastic material.

The safety factors in Fig. 10 may vary if the flexural rigidity  $EI$  of the sheet pile is different. Figure 11 shows the relationship between the safety factor and  $EI$  for the case where the depth of the embedment is 5 m. As shown in this figure, the factor of safety remains almost constant if  $EI$  is large enough. On the other hand, if  $EI$  is less than approximately  $1000 \text{ tf}\cdot\text{m}^2$ , the safety factor decreases gradually and it becomes equal to the safety factor for the case without a sheet pile when  $EI$  approaches infinitely small. Conventional limit analyses can never give this kind of useful information on the effect of a sheet pile in preventing the slope failure. Thus, finite element analysis appears to be a powerful tool for the limit analysis in soil mechanics.

### 3. Adaptive Refinement

#### 3.1 Error estimate and Adaptive analysis

In the previous section, it was shown that the finite element method can give satisfactory results in the limit analysis in soil mechanics. However, there are some cases where the finite element analysis gives limit values that are too large. This is due to the fact that the mesh division is too coarse, especially near the stress singularity point such as the corner of the vertical slope. Mesh refinement is necessary to improve such results. Mesh refinement has been carried out based on a mixture of experience, intuition and guesswork and its validity was verified by the comparison with the closed form solutions. However, new procedure called the adaptive analysis was developed for improving finite element results<sup>4)</sup>.

In the adaptive finite element procedure, the results are successively refined based on accuracy estimates. Thus, how to estimate the accuracy and/or the error is a key to the analysis. Most of the methods of error estimate involve in the energy norm evaluation of integrals interelement stress discontinuities. We have difficulties in implementing this error estimate to usual finite element codes because it requires

explicit determination of the interelement traction jumps and an integration along element interfaces. Another error estimate procedure was developed by Zienkiewicz et al.<sup>5)</sup>. In this method, the error is easily estimated based on usual finite element procedures as will be described below.

Let us consider a linear elastic problem which is described by the following differential equation.

$$Lu + p = 0$$

where  $L$  is a suitable linear operator and  $u$  is displacement. In the finite element method, we obtain approximate solution of the original differential equation by minimizing the potential energy. The final equation is expressed by the following equation in a matrix form<sup>6)</sup>.

$$\int B^T \sigma = f$$

approximate stress  $\hat{\sigma}$  is obtained by elasticity matrix  $D$  and approximate strain  $\epsilon$

$$\hat{\sigma} = D\epsilon$$

strain is derived from nodal displacements  $\bar{u}$  and shape function  $N$

$$\epsilon = N\bar{u}$$

The error is defined as the difference between the approximate values  $\bar{u}, \hat{\sigma}$  and the exact values  $u, \sigma$ .

Thus, we have the error in stress  $e_\sigma$

$$e_\sigma = \hat{\sigma} - \sigma$$

We cannot obtain the exact stress except for simple problems where closed form solutions are available. However, if we can obtain a better approximation than  $\hat{\sigma}$ , we may use it to estimate the error. To calculate better approximation in stress, Zienkiewicz et al. proposed to use nodal stresses and displacement shape function  $N$ . By the weighted residual method, the following equation can be derived.

$$\int N^T (\sigma^* - \sigma) d\Omega = 0$$

because nodal stress  $\sigma^*$  is expressed by the nodal stress  $\bar{\sigma}^*$  and the shape function  $N$

$$\sigma^* = N\bar{\sigma}^*$$

we can obtain  $\sigma^*$  as

$$\sigma^* = A^{-1} \int N^T D S N d\Omega \bar{u}$$

where

$$A = \int N^T N d\Omega$$

we can use as a better approximation to obtain the error

$$e_\sigma = \sigma^* - \hat{\sigma}$$

It was made clear that by using the procedure described above, we can evaluate the error successfully. In fact, it was shown that this procedure is approximately equivalent to the method in which interelement stress discontinuities are integrated. Furthermore this procedure can be implemented to usual finite element program quite easily.

Now that we can estimate the error, the next step is how to make mesh refinement. There are two main strategies in mesh refinement. The first is the simple reduction of the subdivision size which is called h-refinement. The second is called p-refinement where the order of shape function is increased. Because the former is simpler and more versatile, we use the former procedure in this report.

### 3.2 Numerical examples

#### (1) Bearing capacity of strip footing on clay

In the previous section, it was shown that fairly accurate  $N_c$  can be obtained by using conventional finite element analysis. For example, the values of  $N_c$  for a smooth footing with  $\nu=0$  is 5.42 as shown in Table 1. Although this value is satisfactory from the engineering point of view compared with  $N_c=5.14$  by the

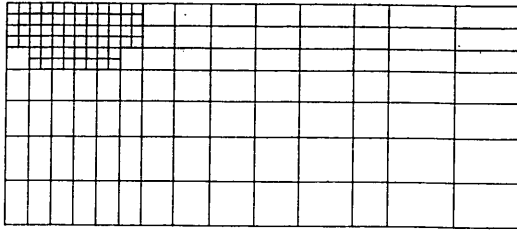


**Fig. 12(a)** Refined mesh 1 for bearing capacity analysis

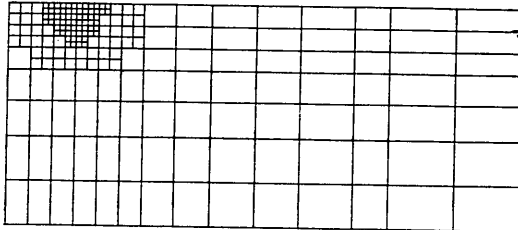


**Fig. 12(b)** Refined mesh 2 for bearing capacity analysis

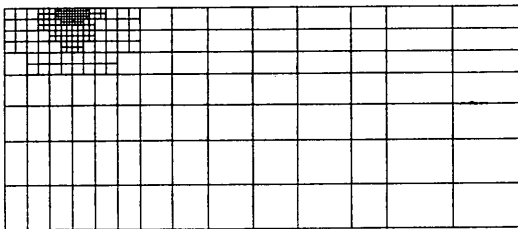


**Fig. 12(c)** Refined mesh 3 for bearing capacity analysis

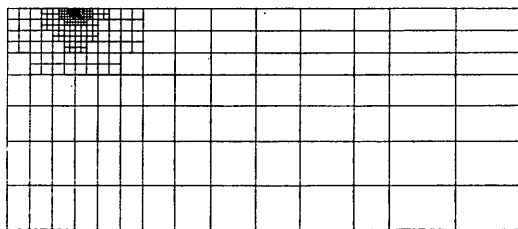


**Fig. 12(d)** Refined mesh 4 for bearing capacity analysis

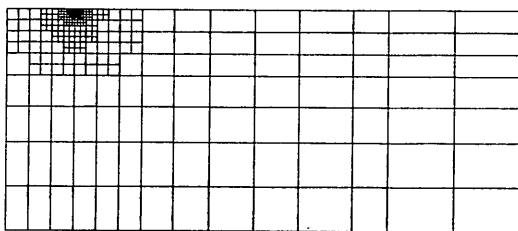


**Fig. 12(e)** Refined mesh 5 for bearing capacity analysis

closed form solution, we can expect more improved value can be obtained by the adaptive analysis.

Figure 12(a) shows a refined mesh based on a error estimate of the original mesh (Fig. 1). Here, about 100 tf/m<sup>2</sup> pressure was applied to the footing and elements whose error in stress exceeds 1 tf/m<sup>2</sup> were refined. In the refinement, isoparametric elements were halved in both horizontal and vertical directions. Using the same strategy, successively refined mesh can be obtained based on the error estimates of the previous mesh as shown in Fig. 12(b)-Fig. 12(e). Because the elements are extremely fine for the mesh 5 and 6, enlarged elements close to the footing edge are shown in Fig. 13.  $N_c$  was newly calculated for 5 mesh of Fig. 12. Table 2 shows the results where error in stress  $S$ ,  $S/A$  which is a normalized error with total area  $A$  and  $N_c$  are compared for 6 cases including the original mesh 0. As shown in this table, extremely accurate  $N_c$ , which is equal to 5.14 of the closed form solution, can be obtained by the adaptive analysis.

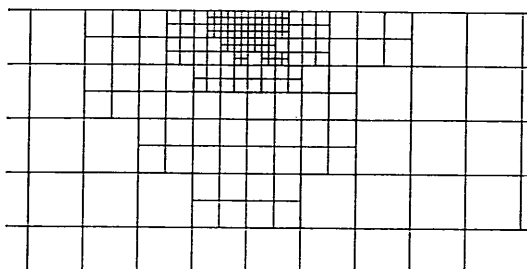


Fig. 13(b) Enlarged mesh 4 for bearing capacity analysis

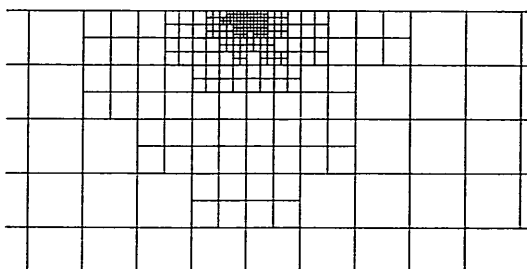


Fig. 13(a) Enlarged mesh 5 for bearing capacity analysis

Table 2 Relationship between stress error and bearing capacity factor  $N_c$

| MESH | $S$   | $S/A$ | $N_c$ |
|------|-------|-------|-------|
| 0    | 125.4 | 2.18  | 5.42  |
| 1    | 78.4  | 1.19  | 5.29  |
| 2    | 36.3  | 0.63  | 5.22  |
| 3    | 15.7  | 0.27  | 5.18  |
| 4    | 7.9   | 0.14  | 5.15  |
| 5    | 4.0   | 0.07  | 5.14  |



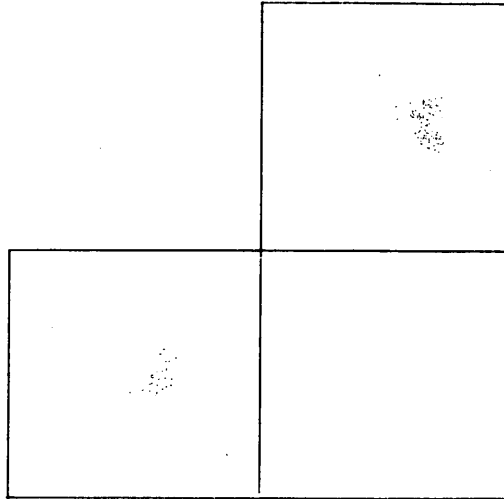


Fig. 14(a) Original mesh 1 for slope stability analysis

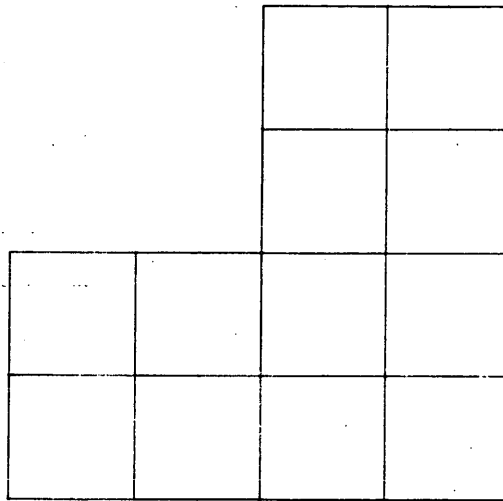


Fig. 14(b) Refined mesh 2 for slope stability analysis

## (2) Stability of vertical slope

In the slope stability analysis, it was shown that the finite element analysis overestimated the safety factor for vertical slopes. This is due to the fact that high stress singularity is observed at the corner of the vertical slopes. To obtain more accurate safety factor, the adaptive analysis was applied to the vertical slope of clay with  $\phi=0$ . Same refinement strategy which was used in the bearing capacity analysis was employed.

Figure 14(a) shows a very simple mesh division which is necessary and yet sufficient to simulate a vertical slope by rectangular elements. The slope height is 20 m in this analysis and necessary parameters are as follows:  $c=20 \text{ tf/m}^2$ ,  $\gamma=$

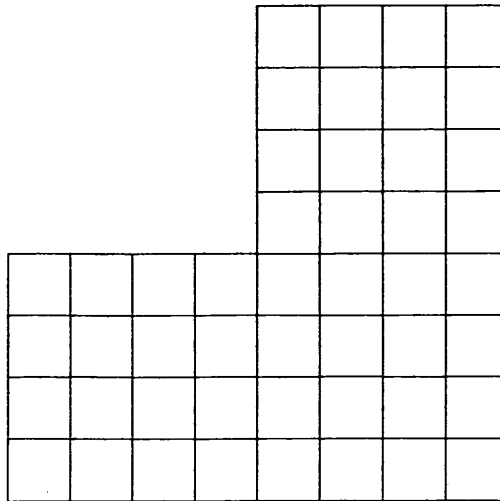


Fig. 14(c) Refined mesh 3 for slope stability analysis

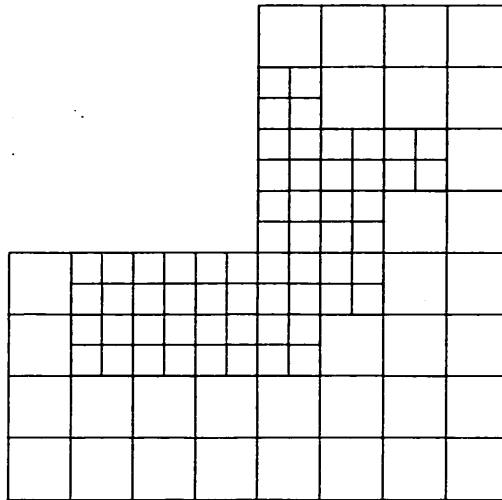


Fig. 14(d) Refined mesh 4 for slope stability analysis

3.83 tf/m<sup>3</sup>,  $E=100$  tf/m<sup>2</sup>,  $\nu=0.3$ . Figure 14(b)-14(f) show refined mesh based on error estimates. Table 3 shows the results of stability factor  $N_s$  and error estimates. In this table, error in stress  $S$  and normalized error  $S/A$  are listed. As shown in this table, exact  $N_s$  value which is equal to 3.83 can be obtained by the adaptive analysis. Furthermore, this example shows the possibility that computers can automatically obtain an appropriate mesh division based on a simple mesh which suffices to simulate both geometric conditions and soil conditions.

#### 4. Conclusion

In this report, it was shown that the finite element method has powerful

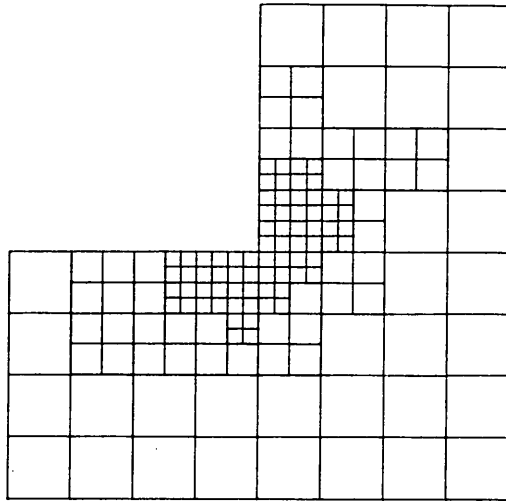


Fig. 14(e) Refined mesh 5 for slope stability analysis

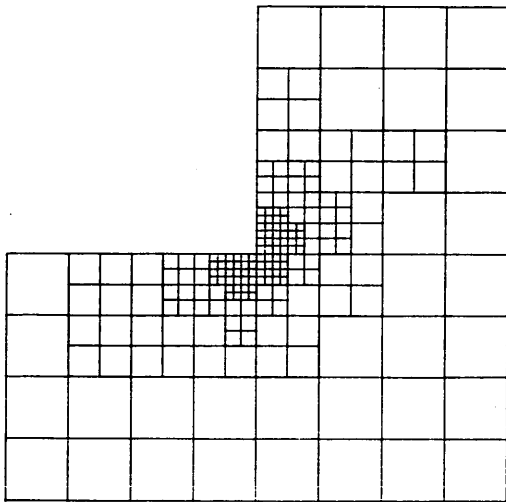


Fig. 14(f) Refined mesh 6 for slope stability analysis

Table 3 Relationship between stress error and stability factor  $N_s$

| MESH | S      | S/A  | $N_s$ |
|------|--------|------|-------|
| 1    | 11,607 | 9.67 | 4.55  |
| 2    | 9,975  | 8.31 | 4.31  |
| 3    | 4,951  | 1.91 | 4.07  |
| 4    | 2,297  | 4.13 | 3.95  |
| 5    | 1,075  | 0.90 | 3.89  |
| 6    | 507    | 0.42 | 3.83  |

capabilities for the limit analysis. Main conclusions can be summarized as follows:

- 1) Elastic parameters  $E$  and  $\nu$  have a negligible effect on the results of the limit analysis in the finite element method.
- 2) The bearing capacity of strip footings was analyzed. The results of the finite elements agreed favourably with the classical bearing capacity equations.
- 3) The stability of simple slopes was analyzed. The finite element method gives higher safety factors for slopes with  $\phi > 0$  whereas it gives favourable agreement with the Taylor's stability chart for slopes with  $\phi = 0$ .
- 4) The effect of a sheet pile on the stability of a slope was analyzed to show the powerful capabilities of the finite element method. The increase of the stability due to the existence of a sheet pile can be analyzed. The effect of its flexural rigidity also can be evaluated.
- 5) Extremely accurate results can be obtained by the adaptive procedure both in the bearing capacity analysis and in the slope stability analysis.

(Received on March 31, 1988)

### Acknowledgements

The author is grateful to Dr. Y. Umehara for his valuable comments on the draft.

### Appendix

- 1) ZIENKIEWICZ, O. C. and CORMEAU, I. C.: Visco-plasticity and creep in elastic-solids—a unified numerical solution approach, *Int. J. Num. Meth. Eng.* Vol. 8, 1974.
- 2) CHEN, W. F.: Limit analysis and soil plasticity, Elsevier, 1975.
- 3) TAYLOR, D. W.: Fundamentals of soil mechanics, Wiley, 1943.
- 4) BABUSKA, I., ZIENKIEWICZ, O. C., GAGO, J. and OLIVEIRA, E. R. deA. (eds.): Accuracy Estimates and adaptive refinement in finite element computations, Wiley, 1986.
- 5) ZIENKIEWICZ, O. C. and ZHU, J.: A simple error estimator and adaptive procedure for practical engineering analysis, *Int. J. Num. Meth. Eng.* Vol. 24, 1987.
- 6) ZIENKIEWICZ, O. C.: The finite element method, 3rd edn., McGraw-Hill, 1977.

### References

It is useful to introduce the following three stress invariants to express the yield criterion.

$$\begin{aligned}\sigma_m &= (\sigma_x + \sigma_y + \sigma_z) \\ \bar{\sigma} &= [(s_x^2 + s_y^2 + s_z^2) + \tau_{xy}^2 + \tau_{yz}^2 + \tau_{zx}^2] \\ \theta &= \frac{1}{3} \sin^{-1} \left[ -\frac{3\sqrt{3}}{2} \cdot \frac{J_3}{\bar{\sigma}^3} \right] \left( -\frac{\pi}{6} < \theta < \frac{\pi}{6} \right)\end{aligned}$$

$$\begin{aligned}\text{where } J_3 &= s_x s_y s_z + 2\tau_{xy} \tau_{yz} \tau_{zx} - s_x \tau_{yz}^2 - s_y \tau_{zx}^2 - s_z \tau_{xy}^2, \quad s_x = \sigma_x - \sigma_m, \quad s_y = \sigma_y - \sigma_m, \\ s_z &= \sigma_z - \sigma_m.\end{aligned}$$

Using these stress invariants, the yield surface  $F$  and the plastic potential  $Q$  of Mohr-Coulomb materials can be written as

$$F = Q = \sigma_m \sin \phi + \sigma \cos \theta - \frac{\sigma}{3} \sin \phi \sin \theta - c \cos \phi$$

In the fictitious viscoplastic algorithm, the flow rule is expressed as

$$\dot{\epsilon}_{vp} = \frac{d\epsilon_{vp}}{dt} = \beta(\sigma)$$

The stress increment can be calculated as follows

$$\Delta\sigma = D(\Delta\epsilon - \Delta t\beta)$$

$$D = [D^{-1} + \Delta S]^{-1}$$

where  $D$  is elastic stress matrix and  $S = (\partial\beta/\partial\sigma)$

$\beta$  is written as

$$\beta = \gamma \left\langle \frac{F}{F_0} \right\rangle \frac{\partial Q}{\partial \sigma}$$

where  $\gamma$  is the fluidity parameter and  $F_0$  is the unit stress

The notation  $\langle \rangle$  implies

$$\langle x \rangle = x \text{ for } x > 0$$

$$\langle x \rangle = x \text{ for } x \leq 0$$

The matrix  $S$  is given as

$$S = \left( \frac{\partial\beta}{\partial\sigma} \right) = \frac{\gamma}{F_0} \left\{ \frac{\partial F}{\partial\sigma} \cdot \frac{\partial Q}{\partial\sigma} + F \frac{\partial^2 Q}{\partial\sigma^2} \right\}$$